HHS Public Access

Author manuscript

Biomaterials. Author manuscript; available in PMC 2018 August 01.

Published in final edited form as:

Biomaterials. 2017 August ; 137: 11–22. doi:10.1016/j.biomaterials.2017.05.019.

Selective targeting and therapy of metastatic and multidrug resistant tumors using a long circulating podophyllotoxin nanoparticle

Aniruddha Roy[1,2], **Yucheng Zhao**[1], **Yang Yang**[1], **Andras Szeitz**[1], **Tara Klassen**[1], and **Shyh-Dar Li**[1,*]

[1]Faculty of Pharmaceutical Sciences, University of British Columbia, Vancouver, BC, Canada V6T 1Z3

[2]Birla Institute of Technology & Science (BITS)-Pilani, Pilani Campus, Vidya Vihar, Pilani, Rajasthan, India 333031

Abstract

Treatment options for metastatic and multidrug resistant (MDR) tumors are limited, and most of the chemotherapeutic drugs exhibit low efficacy against MDR cancers. An anti-tubulin agent podophyllotoxin (PPT) displays high potency against MDR tumor cells. However, due to its poor solubility and non-specificity, PPT cannot be used systemically. We have developed a self-assembling nanoparticle dosage form for PPT (named Celludo) by covalently conjugating PPT and polyethylene glycol (PEG) to acetylated carboxymethyl cellulose (CMC-Ac) via ester linkages. Celludo displayed extended blood circulation with an 18-fold prolonged half-life ($t_{1/2}$), 9,000-fold higher area under the curve (AUC), and 1,000-fold reduced clearance compared to free PPT. Tumor delivery was 500-fold higher in the Cellduo group compared to free PPT. Against the lung metastatic model of EMT6-AR1, Celludo showed selective localization in the metastatic nodules and increased the median survival to 20 d compared to 6-8 d with docetaxel and PPT treatment. In the intraperitoneal metastatic model of human ovarian NCI-ADR/RES tumor, Celludo prolonged the median survival from 50 d to 70 d, whereas the standard therapy PEGylated liposomal doxorubicin showed no effect. No major toxicity was detected with the Celludo treatment. These results demonstrate that Celludo is effective against metastatic and MDR tumors.

Keywords

Podophyllotoxin; Nanoparticles; Multidrug resistance; Metastatic cancer; Drug delivery

*Corresponding author: 2405 Wesbrook Mall, Vancouver, BC, Canada V6T 1Z3, shyh-dar.li@ubc.ca, TEL: 1-604-827-0675.

1. Introduction

Although early detection and novel therapeutic modalities has improved treatment of some cancers, no significant reduction in the mortality rate has been reported for majority of the advanced cancers that have developed metastases, including lung, prostate, colorectal and ovarian cancer [1]. In many of these cases, the tumors initially respond to chemotherapy and exhibit reduction in the mass, but they eventually relapse and become resistant to chemotherapy. During this period, many diseases develop into the metastatic stage. Treatment options are limited for these resistant and metastatic tumors, posing a formidable challenge. There are many mechanisms for the development of resistance in tumor cells, and the most studied and prevalent one is the over-expression of the membrane efflux pump, P-glycoprotein (Pgp) [2]. The majority of the commonly used chemotherapeutic drugs are substrates for Pgp, such as taxanes, vinca alkaloids, anthracyclines and epi-podophyllotoxins, hence are ineffective against Pgp over-expressing tumors [3, 4]. Apart from drug resistance, effective delivery of chemotherapeutics to metastatic tumors remains a major challenge. Increasing dose of the drug has limited effect and in many instances drug toxicity becomes the limiting factor for the treatment of these patients [5]. The 5-year survival rate for localized breast cancer is 99%, but that declines to 24% for metastatic diseases [1]. For colorectal cancer, the 5-year survival rate is 90% when detected at a localized stage, and it reduces to 13% after tumors metastasize [1]. At the metastatic stages, surgery is no longer an effective treatment, and as most of the advanced metastatic tumors have developed multidrug resistance (MDR) [6, 7], an effective therapy must be safe and can overcome the major MDR mechanisms such as Pgp overexpression. We have previously demonstrated that podophyllotoxin (PPT) is a potent drug against a panel of MDR tumor cells with an IC50 ~10 nM [8]. PPT is a natural product extracted from roots and rhizomes of Podophyllum species and is an anti-tubulin agent acting on the cholchicine-binding site in the tubulin, preventing the polymerization, which leads to mitotic arrest and cellular apoptosis [9]. PPT thus remains active against tumors that overexpress β-III tubulin [10]. However, PPT cannot be used systemically due to its poor solubility and selectivity, inducing significant side effects with a low maximum tolerated dose (MTD, 20 mg/kg in mice) [8]. It has been demonstrated that tumor vasculature is highly permeable, and nanoparticles (NP) can selectively accumulate in tumor tissues [11]. Furthermore, lymphatic drainage in tumors is usually compromised, and as a result, NPs can readily enter but cannot exit the tumor compartment [12]. This enhanced permeability and retention (EPR) effect of NPs provides a significant advantage over small molecule drugs. Additionally, NPs provide a detergent and solvent free formulation for drugs that are water insoluble. We have thus developed a NP drug delivery system for PPT, and this system (named Celludo) increased the PPT dose that could be safely administered to mice, resulting in enhanced efficacy in mice bearing different s.c. MDR tumors [8]. The previous work also reported the tissue distribution of the fluorescently labeled Celludo NPs [8], however the results were based on the dye that was passively loaded into Celludo NPs, but not PPT delivery. This manuscript focuses on comparing the pharmacokinetics and biodistribution of free PPT and Celludo. The efficacy of Celludo against metastatic and MDR tumor models was also examined in comparison with the standard therapies. Toxicology study was also performed to examine the safety of Celludo.

2. Materials and methods

2.1. Materials and reagents

Podophyllotoxin (PPT) was purchased from Carbosynth Limited (Compton, Berkshire, UK). Docetaxel (DTX) and Paclitaxel (PTX) were obtained from LC Laboratories (Woburn, MA). Doxorubicin (DOX) was purchased from Tocris Bioscience (Ellisville, MO). Poly(ethylene glycol) methyl ether (mPEG–OH, MW = 2000; no polydispersity index (PDI) data available), 1-ethyl-3-(3-dimethylaminopropyl)-carbodiimide HCl (EDC.HCl), and 4-dimethylaminopyridine (DMAP) were purchased from Sigma Aldrich (Oakville, ON, Canada). Hydrophobic fluorescent dye DiI (1,1′-dioctadecyl-3,3,3′,3′-tetramethylindocarbocyanine perchlorate, D-307) was purchased from Invitrogen (Burlington, ON, Canada). Ammonium formate was purchased from Sigma-Aldrich (St. Louis, MO). Methyl-tert-butyl ether, acetonitrile, and methanol (HPLC grade) were purchased from Fisher Scientific (Fair Lawn, NY), hydrochloric acid (1.0 M) from VWR (West Chester, PA). Ultra pure water was prepared using Milli-Q Synthesis system (Millipore, Billerrica, MA). Sodium carboxymethylcellulose (CMC) (CEKOL 30000, degree of substitution = 0.82 was received from CPKelco (Atlanta, GA). Slide-a-Lyzer dialysis cartridges were purchased from pierce Biotechnology (Rockford, IL). Vivaspin 10 kDa MWCO ultracentrifugation filters were purchased from Fisher Scientific (Ottawa, ON, Canada). Formic acid (99.99%) and morpholine (99.99%) were purchased from Sigma-Aldrich (Oakville, ON, Canada). Blank BALB/c mouse plasma and liver homogenate were purchased from Bioreclamation IVT (Chestertown, NY). Homogenate Navy RINO Lysis kit 50 for sample homogenizing was purchased from FroggaBio Inc (Toronto, ON, Canada). All other general laboratory chemicals were purchased from Fisher Scientific Fisher Scientific (Ottawa, ON, Canada) and VWR scientific (Mississauga, ON, Canada). Resistant EMT6/AR1 cells overexpressing P-glycoprotein (Pgp) were a gift from Dr. Ian Tannock (Princess Margaret Hospital, Toronto, ON, Canada). NCI-ADR/RES cells were obtained from National Cancer Institute (Frederick, MD).

2.2. Synthesis and preparation of Celludo nanoparticles (NPs)

Celludo NPs were prepared as described previously [8]. Briefly, m-PEG-OH and PPT were conjugated to acetylated carboxymethyl cellulose (CMC-Ac) via EDC/DMAP coupling chemistry. CMC-Ac (300 mg, 1.2 mmol acid) was weighed into a 25 mL round bottom flask, and dissolved in a mixture of anhydrous MeCN (9 mL) and DMSO (6 mL). EDC HCl (448 mg, 2.4 mmol) and DMAP (580 mg, 4.8 mmol) were added into that solution followed by addition of PPT (340 mg, 0.8 mmol) and m-PEG-OH (1200 mg, 0.6 mmol). After an overnight reaction, the mixture was precipitated through 135 mL diethyl ether. The precipitate was dried, re-dissolved in MeCN, and the precipitation process was repeated twice. The final precipitate was dried under vacuum, and dialyzed (MW cut-off = 10 kDa) against MilliQ water for 24 h with 3 changes. It was then lyophilized into a dry powder form. The NPs were prepared by the nano-precipitation method using a microfluidic mixing device NanoAssemblr (Precision Nanosystems International, Vancouver, BC, Canada). Thirty mg of the polymer conjugate was dissolved in 1 mL MeCN and precipitated into 3 mL of normal saline in the NanoAssemblr at a flow rate of 18 mL/min. The formed particles were dialyzed in a Slide-A-Lyzer 10,000 MWCO cartridge against 0.9% saline for overnight

to extract solvent. The particles were filtered through a 0.22 μm Millipore PVDF filter, and were concentrated using a Vivaspin unit (10,000 MWCO). Particle size and zeta potential were measured with a Zetasizer (Nano-ZS, Malvern Instruments, Malvern, UK). PPT content in the NPs was determined by ^{1}H-NMR using 2-methyl 5-nitro benzoic acid as an internal standard. DiI loaded NPs were prepared by dissolving 30 mg of the polymer in MeCN (1 mL) containing 0.1 mg/mL DiI and was precipitated into 3 mL of normal saline in the NanoAssemblr at the flow rate of 18 mL/min. DiI content of the NPs was determined by dissolving the NPs in DMSO and assaying for fluorescence (Excitation filter: 535 nm; Emission Filter 590 nm) and comparing to a calibration curve of fluorescence versus DiI concentration, subtracting the background signal of un-loaded particle fluorescence.

2.3. Determination of critical aggregation concentration (CAC)

CAC of Celludo was determined by using the fluorescence depolarization method [13]. Briefly, 1,6-Diphenyl-1,3,5-hextriene (DPH, 1.175 mg) was dissolved in MeCN (10 mL) to form a stock solution. Celludo polymer (10 mg) was serially diluted with the DPH solution to form a series of 10 concentrations of Celludo (1, 0.5, 0.25, 0.05, 0.025, 0.005, 0.0025, 0.0005, 0.00025, 0.00005 mg/ml) in a constant concentration of DPH, 100 μL of each sample were precipitated dropwise in 900 μL normal saline on a vortexer at room temperature for 1 min. One hundred μL of each particle solution was transferred to a 96-well microplate, and fluorescence was measured (Ex 360 nm, Em 460 nm) on a plate reader.

2.4. Instrumentation and experimental conditions

Plasma and tissue concentrations of Celludo and free PPT were determined by an ultra high performance liquid chromatography-tandem mass spectrometry (UHPLC/MS/MS) method using cabazitaxel (CBZ) as an internal standard (IS). The UHPLC/MS/MS system consisted of an Agilent 1290 Infinity Binary Pump, a 1290 Infinity Sampler, a 1290 Infinity Thermostat, and a 1290 Infinity Thermostatted Column Compartment (Agilent, Mississauga, ON, Canada) connected to an AB Sciex QTrap® 5500 hybrid linear ion-trap triple quadrupole mass spectrometer equipped with a Turbo Spray source (AB Sciex, Concord, ON, Canada). The mass spectrometer was operated in positive ionization mode and data were acquired using the Analyst 1.5.2. software on a Microsoft Windows XP Professional operating platform.

Chromatographic analyses were performed using a Waters Acquity UPLC BEH C18, 1.7 μm 2.1 × 50 mm column, which was protected by a Waters Acquity UPLC BEH C18 VanGuard guard column (1.7 μm, 2.1 × 5 mm) (Waters Corp., Milford, MA). The columns were maintained at 30 °C and the auto sampler tray temperature was maintained at 10 °C. Solvent A was water with 2.5 mM ammonium formate (AF), solvent B was methanol with 2.5 mM AF. The mobile phase initial conditions were solvent A (50%) and solvent B (50%), which was ramped to solvent A (5%) by 1.3 min, held until 3.0 min and followed by an equilibration with solvent A (50%) and solvent B (50%) for 2 min. The flow rate was 0.2 mL/min, injection volume was 5 μL with a total run time of 5.0 min. The mobile phase flow was diverted to the waste before 1.4 min and after 3.4 min during the chromatographic run. Mass spectrometric conditions were as follows: curtain gas 30 units, collision gas (CAD) high, ionspray 5500 V, temperature 450 °C, ion source gas 1, 40 units, ion source gas 2, 60

units. Nitrogen gas was used for curtain gas, collision gas, ion source gas 2 (vaporizing gas), and zero air was used for ion source gas 1 (nebulizing gas), entrance potential 10 units, resolution Q1 unit, resolution Q3 unit, and dwell time was 150 msec. PPT and CBZ were monitored using the total ion current (TIC) of the multiple reaction monitoring (MRM) transitions as follows. For PPT (declustering potential DP, 146, collision energy CE, 13, collision cell exit potential CXP, 16), *m/z* 415.3 → 397.1, (DP, 156. CE, 25, CXP, 12) *m/z* 415.3 → 313.0, (DP, 151, CE, 19, CXP, 10), *m/z* 415.3 → 247.1; for CBZ, (DP, 101, CE, 17, CXP, 12), *m/z* 836.5 → 730.4, (DP, 111, CE, 21, CXP, 14), *m/z* 836.5 → 433.2). Using the current experimental conditions, the chromatographic retention time for PPT and CBZ was 2.12 min and 2.66 min, respectively.

2.5. Pharmacokinetic (PK) and biodistribution (BD) study

Female BALB/c mice (6-week old, 18-20 g) were purchased from The Jackson Laboratory (Bar Harbor, ME). The experimental protocols in this study were approved by the Animal Care Committee of the University of British Columbia (Vancouver, BC, Canada) in accordance with the policies established in the Guide to the Care and Use of Experimental Animals prepared by the Canadian Council of Animal Care. EMT-6 AR1 cells (2×10 cells/100 μl media) were s.c. inoculated into the shaved right lateral flank of BALB/c mice. When the tumors reached ~150 mm^3 in diameter, free PPT (20 mg/kg) and Celludo (180 mg PPT/kg) were administrated by an i.v. injection through the tail vein, and blood samples were collected by saphenous vein puncture at selected time-points (6-96 h). Free PPT and Celludo were compared at their MTD and maximum deliverable dose, respectively, which were previously established [8]. Blood samples were collected in EDTA-containing tubes, and spun at 2,500 rpm for 10 min to isolate plasma, which was frozen at -80°C until analysis. Mice were euthanized at 96 h after treatment, and tissues were harvested, rinsed in buffer, and frozen at -80 °C until analysis. PK parameters were calculated with SAAM II (Saam Institute, University of Washington, Seattle, WA) software, using one-compartmentalized data analysis.

2.6. Preparation of calibration standards for the analysis of free PPT

A series of working stock solutions of PPT were prepared in methanol and used for the calibration standards in mouse plasma. The calibration standards were prepared by pipetting 10 μL of blank mouse plasma into a microtube, adding 100 μL of water and spiking it with 10 μL of a working stock solution of PPT. Twenty μL of 20% formic acid (FA) solution was then added. The standards were further processed as described in the sample preparation section (Section 2.7). A calibration curves was prepared freshly on the day of a batch analysis in the concentrations of 5-5,000 ng PPT/mL.

2.7. Preparation of calibration standards for the analysis of Celludo

Analysis of coupled PPT in Celludo required treatment of the NP with morpholine to hydrolyze the ester bonds and liberate PPT. The standards for coupled PPT in Celludo were prepared by a serial dilution of the Celludo NP solution in the range of 500 ng PPT/mL to 0.5 mg PPT/mL in mouse plasma. The calibration standards were prepared by pipetting 10 μL of blank mouse plasma into a microtube and spiking 10 μL of a working stock solution

into the tube, followed by the addition of 10 μL of 250 mM morpholine solution and 100 μL water. The mixture was incubated at 37 °C for 30 h. Subsequently, 20 μL of 20% FA was added to quench the reaction. The standards were further processed as described in the sample preparation section (Section 2.7). A calibration curve was prepared freshly on the day of a batch analysis in the concentration of 0.5-250 μg PPT/ml in mouse plasma.

2.8. Sample preparation

Tissues were homogenized in water (~100 mg in 0.5 ml water) using the Navy bead lysis kit (FroggaBio, Toronto. ON) and the Bullet Blender® Gold (Next Advance, Averill Park, NY). A 10 μL aliquot was transferred to a glass vial and combined with 100 μL water, 10 μL blank plasma or liver homogenates and 10 μL of the 250 mM morpholine solution. The mixture was incubated at 37 °C for 2 h. Subsequently, 50 μL of the 5 μg/mL CBZ IS solution, and 2 ml methyl tert-butyl ether were added. The mixture was vortex-mixed for 30 s and then stored at -80 °C for 10 min. The top (organic) layer was transferred to a microtube, and was brought to dryness in a Zymark TurboVap LV sample evaporator (Zymark Corporation, Hopkinton, MA), under a gentle flow of nitrogen, at 35°C, and the dried residues were reconstituted with 100 μL of water : methanol, 50 : 50 (vol/vol) mixture containing 2.5 mM FA.

2.9. Efficacy against lung metastatic tumor model of EMT6-AR1

To establish the experimental lung metastasis model, 1×10^5 EMT6-AR1 cells were intravenously injected into female BALB/c mice through tail vain. To examine Celludo targeting to metastatic tumor nodules in the lung, DiI labelled Celludo NPs were intravenously administered at the dose of 0.2 μg DiI/animal 1 week post tumor inoculation. After 48 h, animals were euthanized and the lungs and liver were harvested and imaged by the Xenogen system. The DiI signal in each sample was quantified using the Xenogen software. A control group of normal mice (no tumor implantation) were also treated with the same dose of DiI-Celludo, and their lungs and liver were imaged by Xenogen as a comparison. The tissues were then frozen in OCT and cryo-sectioned in 5 μm thick sections. To detect the presence of tumor cells, the tissue sections were stained with FITC-conjugated anti-Ki67 antibody (proliferative tumor cells) and counter-stained with DAPI (nuclei) using similar protocols as described previously [14]. The stained sections were then imaged by a confocal microscope (Zeiss, LSM 700) at 20X magnification. The images were analyzed using ZEN software to examine the specific delivery of DiI-Celludo within the tumor-bearing lung.

For studying efficacy of Celludo against this tumor model, mice were intravenously injected with 1×10^5 EMT6-AR1 cells and were randomly divided into 4 groups. After 3 days of tumor implantation, mice were treated i.v. with either saline (control), MTD of PPT (20 mg/kg; day 0, 4 and 8), MTD of DTX (12 mg/kg; day 0, 4 and 8), and maximum deliverable dose of Celludo (180 mg PPT/kg; day 0, 4 and 8). Animals were monitored using an established clinical scoring sheet (Supplementary Table 1). Animals that reached humane endpoints indicated in Supplementary Table 1 were euthanized and the survival was recorded. Three animals were randomly selected from each group and euthanized at day 10 post treatment, and their lungs were harvested and fixed in 10% formalin. Lungs were then

sectioned, stained with hematoxylin & eosin and imaged with an Aperio Scanner. Image analysis was performed with the Tissue Studio (Definiens Health Image Intelligence).

2.10. Efficacy against intraperitoneal metastasis model of ovarian cancer

Intraperitoneal metastases of MDR ovarian cancer were established by intraperitoneal injection of 1×10^7 NCI-ADR-RES cells into SCID mice. Three weeks later, animals were randomly assigned to receive either saline (control), PPT (20 mg/kg; day 0, 4 and 8), PTX (20 mg/kg; day 0, 4 and 8), PEGylated liposomal doxorubicin (PLD, 5 mg/kg; day 0, 4 and 8) or Celludo (180 mg PPT/kg; day 0, 4 and 8). Again, PPT, PTX and PLD were given at their MTDs established in the lab, and Celludo was dosed at the maximum deliverable dose due to the limit of solubility. Animals were monitored using a clinical scoring sheet (Supplementary Table 1), and animals that reach humane endpoints were euthanized and the survival was recorded.

2.11. Celludo toxicology study

Female BALB/c mice were i.v. treated with Celludo at 180 mg PPT/kg on day 0, 4 and 8, and the toxicity was evaluated using panels of hematology, blood biochemistry, and tissue histology. Mice without any treatment were used as control. Animals were weighed and their general behaviors were monitored using the clinical scoring sheet (Supplementary Table 1).

Blood, serum and tissues samples were collected 1 day post the final dose (day 9) for analysis at the Centre for Comparative Medicine at University of British Columbia (Vancouver, BC, Canada). Mice were anesthetized by isoflurane followed by cervical dislocation for euthanasia. Blood smears were prepared by mounting a drop of blood on one end of a slide, then dispersing the blood along the length of the slide. The slide was dried at room temperature, and then stained with hematoxylin and eosin. Blood samples were sent to Idexx for General Panel (clinical blood chemistry and biochemistry). Harvested tissues were fixed in 10% formalin followed by paraffin embedding, and hematoxylin/eosin staining for histological analysis. Tissue histology was analyzed by a certified animal pathologist at the Centre for Comparative Medicine.

2.12. Statistical analysis

All data are expressed as mean ± SD. Statistical analysis was conducted with the two-tailed unpaired t test for two group comparison or one-way ANOVA, followed by the Turkey multiple comparison test by GraphPad Prism (for three or more groups). A difference with $p < 0.05$ was considered to be statistically significant.

3. Results and discussion

3.1. Preparation and characterization of Celludo

In the first stage of synthesis, sodium carboxymethylcellulose (CMC) was acetylated to make acetylated-CMC (CMC-Ac). The MW of CMC-Ac was 6.5 KDa (error = 2.2%) measured in the batch mode by a multi-angle light scattering (MALS) detector. It was not possible to obtain PDI for this polymer as CMC-Ac stuck tightly to all the size exclusion columns we have tested. CMC-Ac was reacted with PPT and m-PEG in the presence of EDC

and DMAP. Carboxylate groups in CMC-Ac were esterified with the hydroxyl groups of PPT and PEG (Fig 1A). The final polymer conjugate was purified by ether precipitation and dialysis. The final Celludo polymer MW was 23.59 KDa (error = 2.4%). By LC/MS analysis (data not shown), each batch of Celludo was verified to be free of unreacted PEG and PPT. Based on the NMR analysis, the Celludo polymer contained 23 mol% PPT (19 wt%) and 14 mol% PEG (39 wt%). The Celludo polymer self-assembled into NPs in normal saline with a median diameter of 20.3 ± 1.8 nm and a polydispersity index of 0.1 ± 0.04 (Fig 1B). The SEM image showed that the morphology of the Celludo NPs was spherical and homogeneous (Fig 1C).

The critical aggregation concentration (CAC) of Celludo was determined by the fluorescence depolarization method using a fluorescence probe 1,6-diphenyl-1,3,5 hexatriene (DPH), which shows an abrupt increase in fluorescence intensity at the CAC. As shown in supplementary figure 1, the CAC of Celludo was found to be 0.025mg/mL.

3.2. PK and BD study

To minimize non-specific tissue uptake of cytotoxic drugs, these drugs can be loaded into NPs that would exhibit preferential tumor accumulation through the EPR effect. However, this mode of drug delivery is highly dependent on the PK of the formulation. NPs accumulate in tumors via the leaky vasculature, which is a slow process. Therefore, NPs must be stable in blood circulation, and must exhibit a long circulating half-life for gradual tumor accumulation [15]. PK profiles of a drug may also depend on the dose [16]. Therefore, it is advised to study the PK of an investigational drug or dosage form at its therapeutic dose. In the current study, we compared PK and BD of free PPT and Celludo at the doses used in the efficacy studies: 20 mg PPT/kg and 180 mg PPT/kg, respectively. The doses were established in a previous study [8], and 20 mg/kg was the MTD for free PPT and 180 mg PPT/kg represents the maximum dose for Celludo that could be i.v. injected into mice due to the limit of solubility. PPT or Celludo was administrated to EMT6-AR1 tumor bearing BALB/c mice by tail vein injection, and blood samples were collected at selected time points and were analyzed for released PPT and total PPT by the UHPLC/MS/MS method.

As shown in Fig 2 and Table 1, Celludo displayed extended blood circulation with an 18-fold prolonged half-life ($t_{1/2}$), 9,000-fold higher area under the curve (AUC), and 1,000-fold reduced clearance compared to free PPT. The PK of Celludo appeared to follow the one-compartment model and extended over 96 h with a half-life of ~12 h, whereas free PPT exhibited a short circulating $t_{1/2}$ of ~0.7 h and was rapidly cleared from the blood in 9 h. Even if we take into account that the total PPT dose delivered via Celludo was 9-fold higher than that delivered via PPT solution, the difference in AUC remained significant. This extended blood circulation of Celludo would increase its tumor accumulation over time. Prolonged circulating time is a highly important factor for passive tumor targeting of nanomedicines. Moreover, extension of circulation half-life also suggests a less frequent dosing regimen compared to a short-lived drug, improving medication compliance.

Next, we studied BD of Celludo and compared it with free PPT. For the BD study, free PPT or Celludo was i.v. injected into tumor bearing BALB/c mice, and after selected time points

animals were sacrificed and different tissues were collected. Amount of total PPT in the tissue was quantified by UHPLC/MS/MS. As free PPT had a decreased circulation half-life and AUC compared to Celludo, its tissue accumulation was found to be significantly lower than that of Celludo (Fig 3A). Corroborating with the PK data, the highest amount of tissue accumulation of free PPT was found 1 h post injection (3-6 μg/g) in all the major tissues including liver, spleen, kidney and tumor. However, levels of PPT declined rapidly in these tissues and at 9h post injection only a minor amount (< 0.3 μg/g) of PPT was detected (Fig 3A). Colon, brain and muscle displayed no uptake of drug throughout the examined period. In contrast, Celludo exhibited significantly higher tissue accumulation than free PPT, and the tissue uptake persisted for 96 h (Fig 3B). In particular, Celludo displayed 500-fold increased tumor delivery compared to free PPT (tumor AUC of free PPT: 24.8 μg×h/g; tumor AUC of Celludo: 13,366 μg×h/g, Fig 3C). After normalization of the dose (as Celludo was given at a 9-fold higher dose compared to free PPT), 56-fold enhanced tumor delivery was measured with Celludo compared to free PPT.

Unlike the free PPT group, the tumor uptake of Celludo persisted for 96 h, and at 96 h the tumor appeared to be the tissue that displayed the highest uptake of Celludo among all (Fig 3B). Interestingly, the tumor uptake of Celludo occurred early, and at 6 h post injection the tumor level of Celludo reached ~120 μg/g. This early tumor uptake was not observed with most of the reported NP systems, which often required at least 24 h to reach a significant level of accumulation. It is plausible that the small size of Celludo (~20 nm) could lead to effective extravasation into the tumor. In addition to the tumor, Celludo also accumulated in the liver, spleen and kidney, reaching the peak at 24-48 h and then declined. In particular, levels of Celludo in the liver rapidly decreased after 24 h with <30 μg/g detected after 48 h, possibly due to extensive metabolic activity in the liver. The overall uptake of Celludo by the kidney was 1.4fold higher compared to the tumor. This result is somewhat unexpected, as the cut-off size for renal clearance of NPs is 6-10 nm and the diameter of Celludo is ~20 nm. The prolonged blood circulation of Celludo (~12 h) indicated that Celludo was not cleared by the renal filtration; and therefore, the increased kidney uptake of Celludo is likely mediated by accumulation of Celludo in the renal tissue. The renal glomerular filtration barrier is a three-layer structure composed of fenestrated glomerular endothelial cells (with pores diameters in the range of 60-80 nm), glomerular basement membrane between the two cellular layers (rich in heparin sulfate and charged proteoglycans which provides size and charge selectivity), and podocytes (with interdigitating foot processes that form filtration slits of 32 nm) [17-19]. A Japanese group in Osaka reported that a negatively charged polymer poly(vinylpyrrolidone-co-dimethyl maleic acid) (PVD) selectively accumulated in the kidney after intravenous injection [20, 21]. It was suggested that negatively charged polymers exhibit significant affinity with the glomerular basement membrane. Celludo is a 20-nm particle formulation composed of a negatively charged backbone polymer CMC. Although the zeta potential of Celludo was neutral (-2 mV), after some drug release, the carboxylate groups would be exposed and the polymer would become negatively charged. It is hypothesized that Celludo (20 nm) would be able to penetrate through the fenestrated glomerular endothelial layer (pore size = 60-80 nm) and significantly interact with the glomerular basement after some drug release to expose the negatively charged carboxylate groups. Relatively low levels of Celludo were detected in the heart and lung (< 65 μg/g) and

the drug content is under the detection limit in the colon, brain and muscle. In the Celludo group, the overall delivery to the tumor was 1.5-, 4.2-, 3.8-, and 1.6-fold higher compared to the liver, lung, heart and spleen, respectively (Supplementary Table 2).

As the dose of PPT injected through Celludo was 9-fold higher compared to that of free PPT, to minimize the dose effect, BD of free PPT and Celludo was also compared in %injected dose (ID)/g tissue and is presented in Supplementary Figure 2. Celludo displayed significantly higher tumor delivery of PPT during the examined period (6-96 h post injection) compared to free PPT, and about 3-5% ID/g of PPT was detected in the tumor with Cellduo treatment. Free PPT, on the other hand, showed low and poor retention in the tumor, with a peak at 1.5% ID/g at 1 h and the tumor uptake rapidly declined to 0.4% ID/g in 9 h. At 96 h following Celludo treatment, the highest amount of drug was detected in the tumor (5% ID/g) followed by kidney (3.4% ID/g), spleen (2.9% ID/g), heart (1.7% ID/g), lung (1.7% ID/g) and liver (0.9% ID/g). The PK/BD data of improved tumor delivery of Celludo supports our previous finding that Celludo was effective in regressing s.c. MDR tumor models in mice [8].

3.3. Celludo delivery to metastatic tumor nodules

Although the BD data showed encouraging tumor-targeted delivery of Celludo in a s.c. tumor model, heterogeneity in clinical tumors poses a significant challenge for tumor delivery of NPs via the EPR effect. Biological barriers within tumors that impede effective delivery of NPs include heterogeneity in vascular permeability and perfusion, presence of a large amount of stroma and high variability in interstitial fluid pressure (IFP) [22]. Tumors with poor vascular permeability and perfusion, a high stroma content and high IFP are resistant to EPR-based drug delivery. Heterogeneity of the above barriers within a tumor often leads to uneven intratumoral distribution of NPs, resulting in disease recurrence [23]. Additionally, NPs that reply only on the EPR effect have been thought to exhibit poor delivery to small metastatic nodules. To analyze tumor delivery and efficacy of Celludo against a more clinically relevant tumor, Celludo delivery to metastatic tumor was studied. Metastatic tumors are highly fatal, and treatment of metastatic and MDR tumors is most challenging. We first established tumor nodules in lungs by intravenously injecting EMT6-AR1 cells into BALB/c mice. EMT6-AR1 is a highly proliferative murine breast cancer cell line which show multi-drug resistance due to overexpression of Pgp [24]. We have evaluated the lung colonization of EMT6-AR1 cells in an initial experiment. After administration of 1×10^5 cells intravenously, animals were sacrificed at regular interval (every 24 h) and different tissues were visually examined under surgical microscopy. Three days post cell implantation, small nodules were found in the lungs.

DiI labeled Celludo NPs were intravenously injected to mice one week post i.v. inoculation of EMT6-AR1 cells. Two days after Celludo-DiI administration, animals were euthanized and the lungs and liver were isolated. They were imaged by the Xenogen system. Only the tumor-bearing lungs and liver were selected for imaging as the liver was shown to be one of the major uptake tissue for Celludo NPs in the BD study. As depicted in Fig 4A&B, significant lung accumulation of the NPs was only detected in mice bearing lung metastases of EMT6-AR1 tumor, and there was little fluorescence measured in the liver, suggesting

high specificity of Celludo targeting to the lung metastases. The average fluorescence of the tumor bearing lung was 4.8×10^8 p/s/cm^2/sr, whereas in the liver the average fluorescence was only 6.2×10^7 p/s/cm^2/sr, depicting ~8-fold higher accumulation in the tumor bearing lung compared to liver. In the control mice that did not have lung metastases, the average fluorescence in the lungs and liver were 3.1×10^7 p/s/cm^2/sr and 6.5×10^7 p/s/cm^2/sr respectively. The data suggest that Celludo NPs specifically target EMT6-AR1 nodules in the lungs. To confirm this, we further examined the microdistribution of Celludo-DiI NPs within the tumor-bearing lungs. The lungs were collected and cryo-sectioned 48 h after the treatment with Celludo-DiI, and were then labeled with FITC-anti Ki67 antibody (proliferative tumor marker, green) and DAPI (nuclei, blue).

As showed in Fig 4C, co-localization was found between Celludo-DiI and anti Ki67-FITC, and Celludo-DiI uptake in the normal lung tissue (Ki67 negative) was low in both the normal and tumor-bearing lungs. Metastatic tumor nodules have abnormal tissue architectures, which could facilitate the effective accumulation of Celludo NPs [25]. As these nodules were small (~2-5 mm in diameter), our data suggest Celludo NPs could efficiently target small metastatic nodules, which could lead to effective therapy of metastatic tumors. To the best of our knowledge, non-ligand targeted NPs relying only on the EPR effect have not shown much success in targeting lung metastasis, and this work with Celludo represents a successful example of EPR-based drug targeting to lung metastases. The mechanism of Celludo targeting lung metastases remains unknown at the present time and could be due to its small size (20 nm). There are few reports available where actively targeted NPs were evaluated for targeting metastatic cancer. For example, Rychahou et al. [30] demonstrated that a modified tri-hand RNA-NP can effectively target cancer cells in major sites of metastasis, such as liver, lymph nodes, and lung. However, due to the structural and physicochemical constraint of the RNA-NPs, it is challenging to load a high amount of drugs in this type of NPs for effective chemotherapy. Li et al. [31] have shown that the anisamide ligand modified NPs exhibited significant accumulation in the lung metastases of melanoma. There are other examples of the active targeting approach for metastatic tumors, including antibody against neu receptor for breast cancer, α(v)β(3) integrin targeting using cRGD peptide and P-selectin and α(v)β(3) duel targeting [32-34]. Active targeting preferentially targets only the specific receptor expressing cancer cells, but tumors are known to be highly heterogeneous [35].

3.4. Efficacy of Celludo against metastatic MDR tumors

Many tumors are detected at advanced stages with significant metastases, and recurrent tumors after initial chemotherapy often become metastatic. Tumors at these stages are difficult to treat and the patients often suffer from a low survival rate. Therefore, it is urgently needed to develop an effective therapy that can treat metastatic MDR tumors.

In the first study, efficacy of Celludo was evaluated against a metastatic breast tumor model. Breast cancer is one of the most common cancers among women. Metastatic breast cancer has a very low 5 year survival rate of only 24% [1]. Therapies for this disease include taxens alone or in combination with doxorubicin, however the response rate remains poor [36]. Lung is a major organ of metastasis from breast cancer. To determine effectiveness of

Celludo therapy against this disease, tumor metastases were established by intravenous implantation of EMT6-AR1 cells in female BALB/c mice. EMT6-AR1 is a highly proliferative, MDR murine breast tumor line which colonizes in the lungs of mice after i.v. delivery. Three days after tumor implantation, animals were randomly divided into 4 groups and treated with either saline (control), PPT (20 mg/kg; day 0, 4 and 8), DTX (12 mg/kg; day 0, 4 and 8), or Celludo (180 mg PPT/kg; day 0, 4 and 8). Both PPT and DTX were given at their MTDs, and Celludo were given at its maximum deliverable dose due to the limit of solubility (~18 mg/ml). Mice were then monitored using a clinical scoring sheet, and were euthanized when humane endpoints were reached.

As shown in Fig 5A, mice treated with saline, DTX, or PPT had a similar median survival of 6-8 days, while that treated with Celludo showed prolong median survival of 20 days. Mice in the control, DTX and PPT groups showed severe and rapid body weight loss (Fig 5B) with visible signs of pain or distress including piloerection, lethargy, and weakness. Celludo therapy appeared to delay the heath deterioration of the mice that showed a rapid decrease of body weight on day 5 (~10%), but the body weight rebound for a week, followed by a gradual decline until the mice reached endpoints. By day 10, all animals except the Celludo group reached endpoints and were euthanized. Lungs from these animals were harvested for tumor analysis after H&E staining with the help of Definiens software (Fig 5C). Three mice from the Celludo group were randomly selected and euthanized, and their lungs were harvested for comparison. As shown in Fig 5D, while more than 70% of the lungs was covered with tumor nodules in control, PPT and DTX groups (control: 76%; PPT: 75%; DTX 71%), tumor burden in the lungs was less than 30% in the Celludo treated group (28%). Celludo prolonged the animal survival by 3-fold compared to other therapies (Fig 5A).

In the second study, we tested Celludo efficacy against metastatic MDR ovarian cancer. While ovarian cancer is the 8th most common cancer among women, it is the fifth leading cause of cancer-related death among women, and is the deadliest of gynecologic cancers with a 5-year survival rate of 27% after metastasis [1]. Majority of ovarian cancer are detected at late stages with widely metastasized diseases in the peritoneal cavity. The standard-of-care treatment is cytoreductive surgery followed by carboplatin chemotherapy in combination with PTX [37]. However this therapy is not very effective and majority of these patients experience disease progression and a multi-drug resistant (MDR) phenotype [37-39]. Treatment for the advanced disease include PEGylated liposomal doxorubicin (PLD), PTX and etoposide, which produce a response rate of only 10-15% and an overall survival of ~12 months [37, 38]. Of these approved drugs, PLD is preferred because of the convenient schedule (every 4 weeks) and lack of neurotoxicity [38]. To evaluate the potential of Celludo for treating this advanced tumor, a metastatic MDR ovarian tumor model was established by intraperitoneal implantation of NCI-ADR-RES human ovarian cancer cells into female SCID mice. NCI-ADR/RES is a highly resistant tumor line and was developed by exposing the parent cells to increasing concentrations of doxorubicin until the cells are completely resistant at 10 μM doxorubicin. After 3 weeks of tumor implantation, animals were randomly assigned to receive either saline (control), PPT (20 mg/kg; day 0, 4 and 8), PTX (20 mg/kg; day 0, 4 and 8), PLD (5 mg/kg; day 0, 4 and 8), or Celludo (180 mg PPT/kg; day 0, 4 and 8). The animals were monitored using a clinical scoring sheet. As

shown in Fig 6A, Celludo significantly increased the median survival of mice from ~50 days to 70 days, while the other therapies including the standard of care PLD showed no activity. Again, all mice except those treated with Celludo showed rapid deterioration of health 4 weeks after the first dose of treatment, and reached endpoints by day 50 (Fig 6B). Cellduo treated mice displayed stable body weight until day 45, followed by relatively gradual weight loss (Fig 6B).

3.5. Toxicology data

In vivo safety of Celludo was further examined in female BALB/c mice after three i.v. doses of maximum deliverable dose of Celludo (day 0, 4, 8; 180mg PPT/kg). Body weight change, visible and/or palpable dermal infection and grooming or impaired mobility were closely monitored every day. An established clinical scoring sheet was used to evaluate the behavioral status of the mice. The mice displayed a mild decrease in body weight (less than 1%) post injection, but the weight rebounded back quickly. This is also reflected in the clinical scores: a marginal increase in clinical score (2-3) is noted after every injection, which came to normal the next day (Fig 7A). It is noted that a cumulative score of 10 necessitate euthanasia, and no mice reached any humane endpoints during the study.

No histological lesion with any of the tissues, neither gross nor pathological abnormality, was observed by a certified animal pathologist in major organs, including heart, lung, liver, spleen, kidney, colon, eyes, and sciatic nerve (Fig 7B).

Hematological and biochemical examination of the blood was done 1 day post the final treatment (day 9). Overall, no significant change was detected, as shown in Table 2 and Table 3. Platelet count (857×10^9/L) and reticulocyte level (177.1×10^3/μL) showed a slight decrease compared to control (platelet: 1368.7×10^9/L; reticulocyte : 391.7×10^3/μL), but are still within the normal range (platelet: $668–1543\times10^9$/L; reticulocyte: $19.5–493.6\times10^3$/μL). Although there is a significant accumulation of Celludo in the kidney, the parameters in the biochemical toxicity studies (urea and creatinine) did not show that Celludo caused any renal toxicity, which is consistent with the histology observation. There were slight elevations of the serum levels of alanine aminotransferase (ALT, 245 U L^{-1}] and; aspartate aminotransferase (AST, 349.8 U L^{-1}) (normal range: 7–227 U L^{-1} for ALT, 37–329 U L^{-1} for AST). As the histology data precluded any liver inflammation or damage, the increased ALT and AST in the serum could be from muscle caused by mild weight loss.

Toxicity of PPT is well documented in the literature [40, 41]. PPT overdose produced significant neurological disturbance as well as clinical signs and symptoms such as vomiting, diarrhea and abnormal hepatic functions [40, 41]. Treatment with Celludo did not induce any of these side effects.

4. Conclusion

PPT has high potency against Pgp overexpressing MDR tumors but its poor solubility and non-specificity prevents its clinical use to treat cancer. A nanoformulation of PPT, named Celludo, was designed to improve the bioavailability and efficacy of PPT. Celludo increased the circulating half-life of PPT by 18-fold and tumor uptake by 500-fold. Against metastatic

MDR tumor models, Celludo exhibited significantly enhanced efficacy compared to native PPT and standard chemotherapeutics. In toxicological studies, no major sign of toxicity was found with Celludo treatment in hematology, serum biochemistry and tissue histology. These encouraging data suggest that Celludo exhibits significant potential as an effective systemic therapy against MDR and metastatic tumors.

Supplementary Material

Refer to Web version on PubMed Central for supplementary material.

Acknowledgments

This research was supported by grants from Canadian Institutes of Health Research, National Institutes of Health and National Science and Engineering Research Council of Canada. SD Li is a recipient of a New Investigator Award from Canadian Institutes of Health Research and holds the Angiotech Professorship in Drug Delivery.

References

1. Siegel R, Ma J, Zou Z, Jemal A. Cancer statistics, 2014. CA: a cancer journal for clinicians. 2014; 64:9–29. [PubMed: 24399786]
2. Gottesman MM, Fojo T, Bates SE. Multidrug resistance in cancer: role of ATP-dependent transporters. Nature reviews Cancer. 2002; 2:48–58. [PubMed: 11902585]
3. Kim RB. Drugs as P-glycoprotein substrates, inhibitors, and inducers. Drug metabolism reviews. 2002; 34:47–54. [PubMed: 11996011]
4. Chen L, Li Y, Yu H, Zhang L, Hou T. Computational models for predicting substrates or inhibitors of P-glycoprotein. Drug discovery today. 2012; 17:343–51. [PubMed: 22119877]
5. Plenderleith IH. Treating the treatment: toxicity of cancer chemotherapy. Canadian family physician Medecin de famille canadien. 1990; 36:1827–30. [PubMed: 21234006]
6. Gonzalez-Angulo AM, Morales-Vasquez F, Hortobagyi GN. Overview of resistance to systemic therapy in patients with breast cancer. Advances in experimental medicine and biology. 2007; 608:1–22. [PubMed: 17993229]
7. Holohan C, Van Schaeybroeck S, Longley DB, Johnston PG. Cancer drug resistance: an evolving paradigm. Nature reviews Cancer. 2013; 13:714–26. [PubMed: 24060863]
8. Roy A, Ernsting MJ, Undzys E, Li SD. A highly tumor-targeted nanoparticle of podophyllotoxin penetrated tumor core and regressed multidrug resistant tumors. Biomaterials. 2015; 52:335–46. [PubMed: 25818440]
9. Imbert TF. Discovery of podophyllotoxins. Biochimie. 1998; 80:207–22. [PubMed: 9615861]
10. Stengel C, Newman SP, Leese MP, Potter BV, Reed MJ, Purohit A. Class III beta-tubulin expression and in vitro resistance to microtubule targeting agents. British journal of cancer. 2010; 102:316–24. [PubMed: 20029418]
11. Matsumura Y, Maeda H. A new concept for macromolecular therapeutics in cancer chemotherapy:mechanism of tumoritropic accumulation of proteins and the antitumor agent smancs. Cancer research. 1986; 46:6387–92. [PubMed: 2946403]
12. Greish K. Enhanced permeability and retention (EPR) effect for anticancer nanomedicine drug targeting. Methods in molecular biology. 2010; 624:25–37. [PubMed: 20217587]
13. Zhang X, Jackson JK, Burt HM. Determination of surfactant critical micelle concentration by a novel fluorescence depolarization technique. Journal of biochemical and biophysical methods. 1996; 31:145–50. [PubMed: 8675957]
14. Ernsting MJ, Hoang B, Lohse I, Undzys E, Cao P, Do T, et al. Targeting of metastasis-promoting tumor-associated fibroblasts and modulation of pancreatic tumor-associated stroma with a carboxymethylcellulose-docetaxel nanoparticle. Journal of controlled release : official journal of the Controlled Release Society. 2015; 206:122–30. [PubMed: 25804872]

15. Blanco E, Shen H, Ferrari M. Principles of nanoparticle design for overcoming biological barriers to drug delivery. Nature biotechnology. 2015; 33:941–51.
16. Lin JH. Dose-dependent pharmacokinetics: experimental observations and theoretical considerations. Biopharmaceutics & drug disposition. 1994; 15:1–31. [PubMed: 8161713]
17. Haraldsson B, Nystrom J, Deen WM. Properties of the glomerular barrier and mechanisms of proteinuria. Physiological reviews. 2008; 88:451–87. [PubMed: 18391170]
18. Brede C, Labhasetwar V. Applications of nanoparticles in the detection and treatment of kidney diseases. Advances in chronic kidney disease. 2013; 20:454–65. [PubMed: 24206598]
19. Ruggiero A, Villa CH, Bander E, Rey DA, Bergkvist M, Batt CA, et al. Paradoxical glomerular filtration of carbon nanotubes. Proceedings of the National Academy of Sciences of the United States of America. 2010; 107:12369–74. [PubMed: 20566862]
20. Kodaira H, Tsutsumi Y, Yoshioka Y, Kamada H, Kaneda Y, Yamamoto Y, et al. The targeting of anionized polyvinylpyrrolidone to the renal system. Biomaterials. 2004; 25:4309–15. [PubMed: 15046921]
21. Yamamoto Y, Tsutsumi Y, Yoshioka Y, Kamada H, Sato-Kamada K, Okamoto T, et al. Poly(vinylpyrrolidone-co-dimethyl maleic acid) as a novel renal targeting carrier. Journal of controlled release : official journal of the Controlled Release Society. 2004; 95:229–37. [PubMed: 14980771]
22. Ernsting MJ, Murakami M, Roy A, Li SD. Factors controlling the pharmacokinetics, biodistribution and intratumoral penetration of nanoparticles. Journal of controlled release : official journal of the Controlled Release Society. 2013; 172:782–94. [PubMed: 24075927]
23. Li L, Sun J, He Z. Deep penetration of nanoparticulate drug delivery systems into tumors: challenges and solutions. Current medicinal chemistry. 2013; 20:2881–91. [PubMed: 23651305]
24. Patel KJ, Tannock IF. The influence of P-glycoprotein expression and its inhibitors on the distribution of doxorubicin in breast tumors. BMC cancer. 2009; 9:356. [PubMed: 19807929]
25. Kumar S, Weaver VM. Mechanics, malignancy, and metastasis: the force journey of a tumor cell. Cancer metastasis reviews. 2009; 28:113–27. [PubMed: 19153673]
26. Yuan F, Dellian M, Fukumura D, Leunig M, Berk DA, Torchilin VP, et al. Vascular permeability in a human tumor xenograft: molecular size dependence and cutoff size. Cancer research. 1995; 55:3752–6. [PubMed: 7641188]
27. Schadlich A, Caysa H, Mueller T, Tenambergen F, Rose C, Gopferich A, et al. Tumor accumulation of NIR fluorescent PEG-PLA nanoparticles: impact of particle size and human xenograft tumor model. ACS nano. 2011; 5:8710–20. [PubMed: 21970766]
28. Lee H, Fonge H, Hoang B, Reilly RM, Allen C. The effects of particle size and molecular targeting on the intratumoral and subcellular distribution of polymeric nanoparticles. Molecular pharmaceutics. 2010; 7:1195–208. [PubMed: 20476759]
29. Cabral H, Matsumoto Y, Mizuno K, Chen Q, Murakami M, Kimura M, et al. Accumulation of sub-100 nm polymeric micelles in poorly permeable tumours depends on size. Nature nanotechnology. 2011; 6:815–23.
30. Rychahou P, Haque F, Shu Y, Zaytseva Y, Weiss HL, Lee EY, et al. Delivery of RNA nanoparticles into colorectal cancer metastases following systemic administration. ACS nano. 2015; 9:1108–16. [PubMed: 25652125]
31. Li SD, Chono S, Huang L. Efficient gene silencing in metastatic tumor by siRNA formulated in surface-modified nanoparticles. Journal of controlled release : official journal of the Controlled Release Society. 2008; 126:77–84. [PubMed: 18083264]
32. Kievit FM, Stephen ZR, Veiseh O, Arami H, Wang T, Lai VP, et al. Targeting of primary breast cancers and metastases in a transgenic mouse model using rationally designed multifunctional SPIONs. ACS nano. 2012; 6:2591–601. [PubMed: 22324543]
33. Peiris PM, Toy R, Doolittle E, Pansky J, Abramowski A, Tam M, et al. Imaging metastasis using an integrin-targeting chain-shaped nanoparticle. ACS nano. 2012; 6:8783–95. [PubMed: 23005348]
34. Doolittle E, Peiris PM, Doron G, Goldberg A, Tucci S, Rao S, et al. Spatiotemporal Targeting of a Dual-Ligand Nanoparticle to Cancer Metastasis. ACS nano. 2015; 9:8012–21. [PubMed: 26203676]

35. Gerlinger M, Rowan AJ, Horswell S, Larkin J, Endesfelder D, Gronroos E, et al. Intratumor heterogeneity and branched evolution revealed by multiregion sequencing. The New England journal of medicine. 2012; 366:883–92. [PubMed: 22397650]

36. Sledge GW, Neuberg D, Bernardo P, Ingle JN, Martino S, Rowinsky EK, et al. Phase III trial of doxorubicin, paclitaxel, and the combination of doxorubicin and paclitaxel as front-line chemotherapy for metastatic breast cancer: an intergroup trial (E1193). Journal of clinical oncology : official journal of the American Society of Clinical Oncology. 2003; 21:588–92. [PubMed: 12586793]

37. Markman M. Current standards of care for chemotherapy of optimally cytoreduced advanced epithelial ovarian cancer. Gynecologic oncology. 2013; 131:241–5. [PubMed: 23726888]

38. Ambrosio AJ, Suzin D, Palmer EL, Penson RT. Vintafolide (EC145) for the treatment of folate-receptor-alpha positive platinum-resistant ovarian cancer. Expert review of clinical pharmacology. 2014; 7:443–50. [PubMed: 24742319]

39. Syrios J, Banerjee S, Kaye SB. Advanced epithelial ovarian cancer: from standard chemotherapy to promising molecular pathway targets--where are we now? Anticancer research. 2014; 34:2069–77. [PubMed: 24778008]

40. Kao WF, Hung DZ, Tsai WJ, Lin KP, Deng JF. Podophyllotoxin intoxication: toxic effect of Bajiaolian in herbal therapeutics. Human & experimental toxicology. 1992; 11:480–7. [PubMed: 1361136]

41. Filley CM, Graff-Richard NR, Lacy JR, Heitner MA, Earnest MP. Neurologic manifestations of podophyllin toxicity. Neurology. 1982; 32:308–11. [PubMed: 7199647]

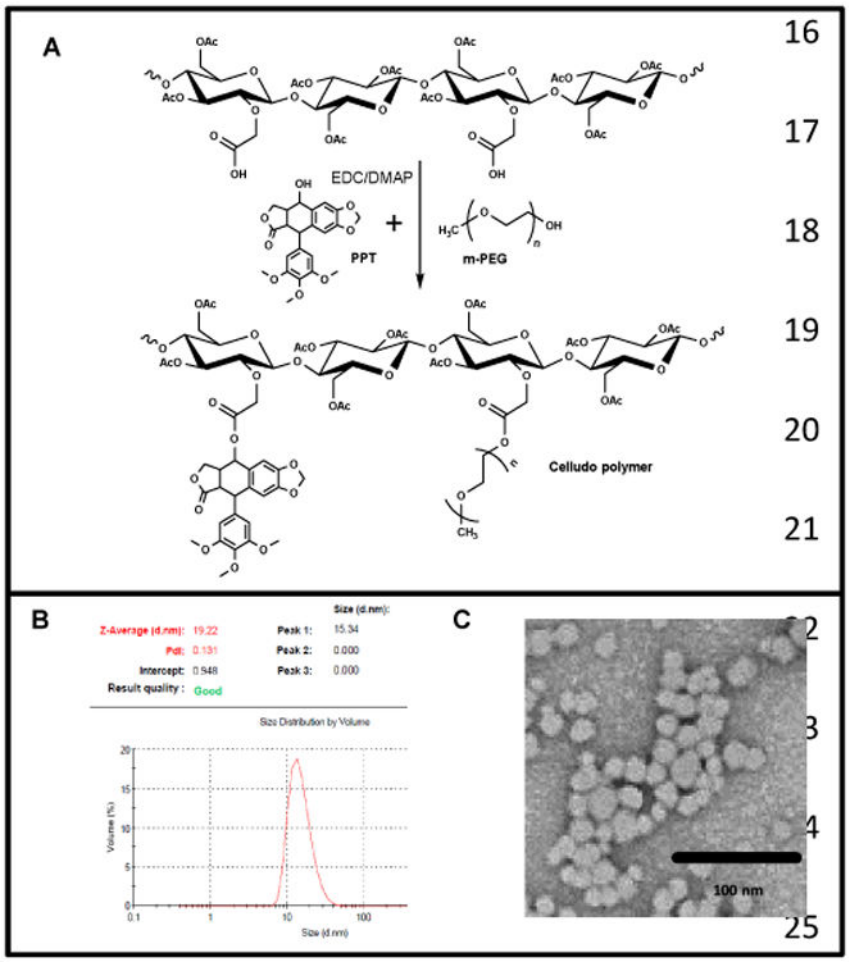

Figure 1.

Synthesis and formation of Celludo NPs. **A**. Synthesis scheme of Celludo polymer. PPT and m-PEG was reacted with CMC-Ac in the presence of EDC and DMAP to produce Celludo polymer. **B**. Size analysis of the Celludo NPs. Celludo NPs had an average size of 20.3 ± 1.8 nm with narrow size distribution and a PDI of 0.1 ± 0.04. **C**. SEM image of Celludo NPs.

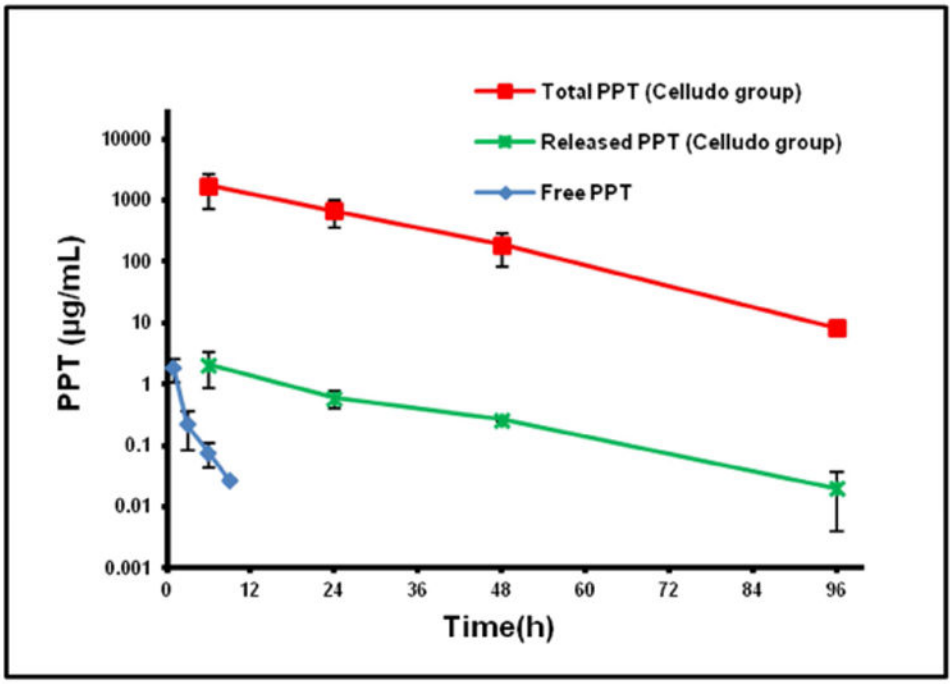

Figure 2.

Pharmacokinetic profiles of free PPT and Celludo in BALB/c mice. Free PPT or Celludo were i.v. administered into BALB/c mice, and the released and total PPT in the plasma was extracted and measured by UHPLC/MS/MS. Data = mean ± SE (n = 3).

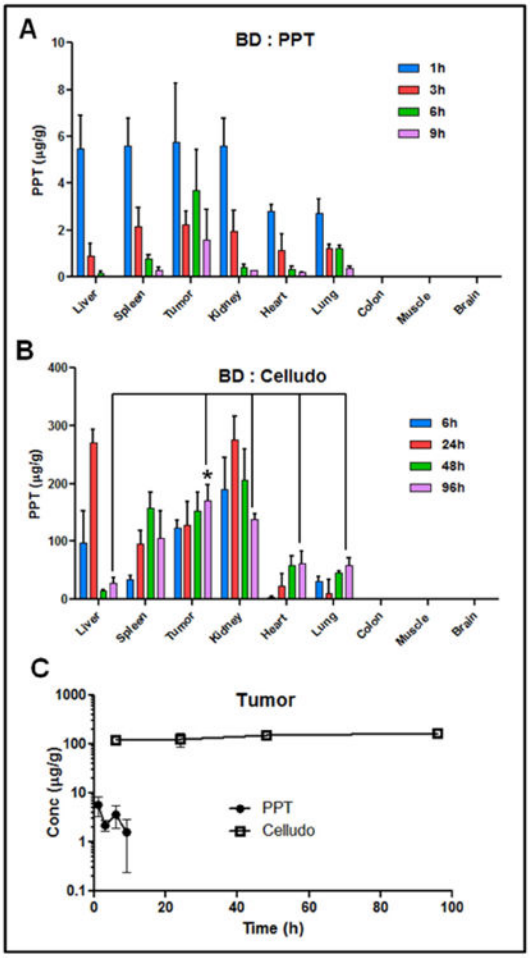

Figure 3.

Biodistribution of PPT delivered as free PPT or Celludo. Free PPT or Celludo was i.v. administered into EMT-6 AR1 tumor bearing BALB/c mice, and the released and total PPT in the tissues were extracted and measured by UHPLC/MS/MS. Data = mean ± SE (n = 3). **A.** BD of free PPT (**inset**: values at lower scale). **B.** BD of Celludo. **C.** Comparison of tumor uptake between free PPT and Celludo. * indicates significant difference ($p < 0.05$).

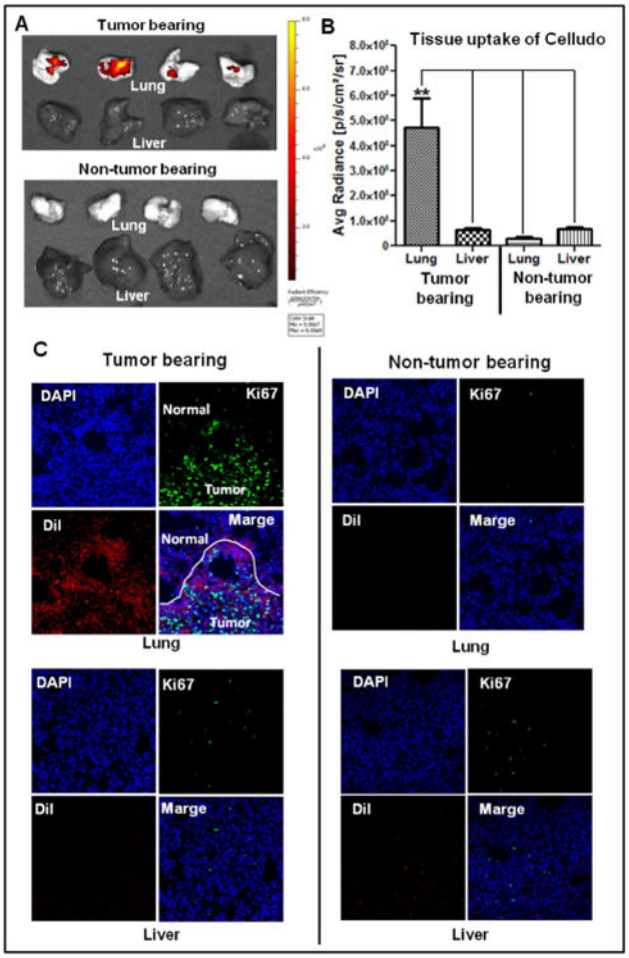

Figure 4.

Targeting of metastatic tumors by Celludo. Metastatic lung tumor was induced by i.v. injection of EMT6-AR1 tumor cells in BALB/c mice. DiI loaded Celludo-NPs were injected i.v. in the normal and tumor bearing mice. After 48h, animals were sacrificed and lung and liver were isolated and imaged. **A**. Whole tissue imaging by the Xenogen system. **B.** Quantitative comparison of Celludo uptake between lung and liver of tumor bearing and non-tumor bearing mice. (** indicates significant difference ($p < 0.01$). **C.** Confocal fluorescence imaging of the tissue sections co-stained with anti-Ki67-FITC antibody (green) and DAPI (blue). Red signal signifies Celludo-DiI.

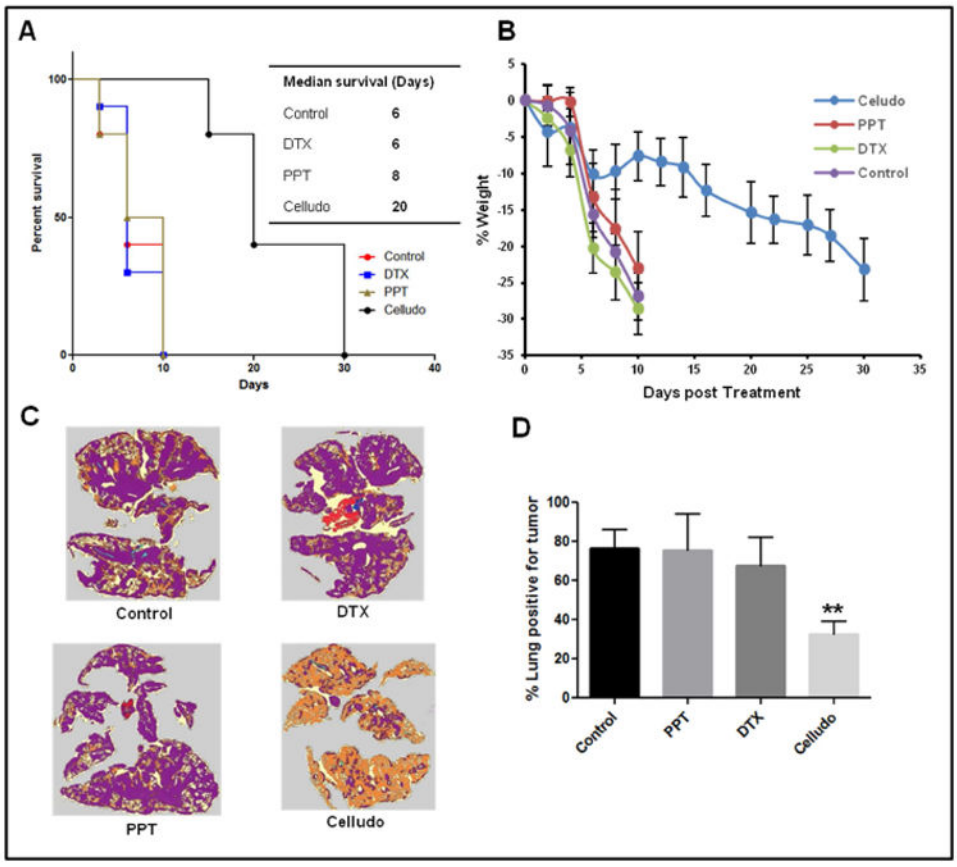

Figure 5.

In vivo efficacy of Celludo against EMT6-AR1 lung metastatic tumor model. EMT6-AR1 cells were implanted i.v. in the female BALB/c mice. Three days after inoculation, mice were treated with either saline, PPT, DTX or Celludo. **A**. Percent survival over time; **B**. Change in body weight. **C**. Definiens image of lung sections of representative animals 10 days post treatment. Violet colour represents tumor nodules. **D**. Quantitative analysis of metastasis in lungs by Definiens software. ** $p < 0.01$ vs control, n=10.

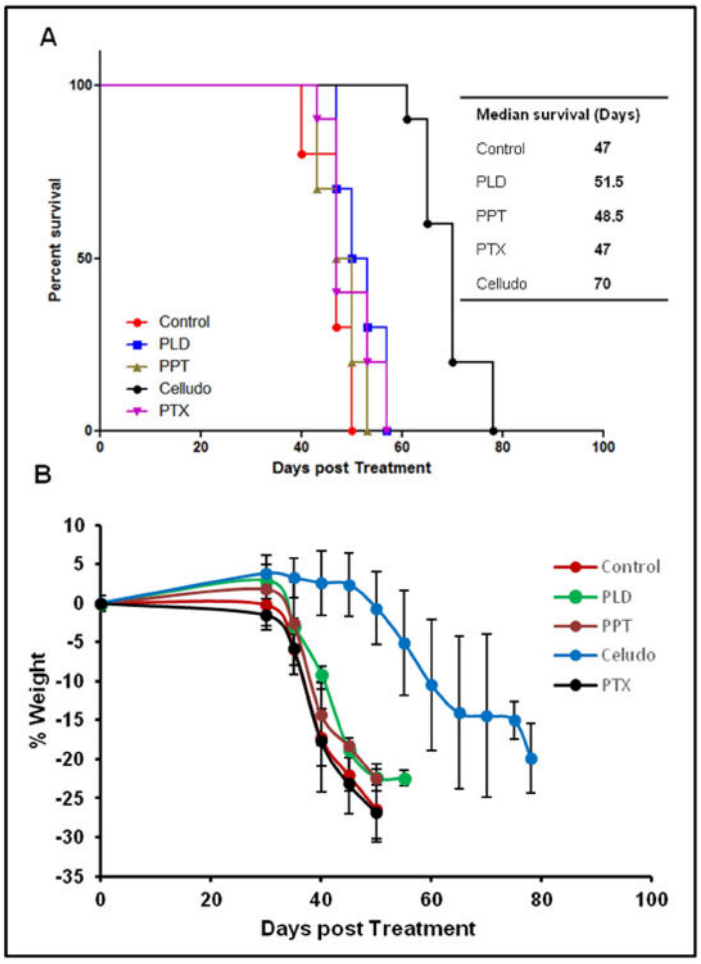

Figure 6.

In vivo efficacy of Celludo against NCI-ADR RES peritoneal metastatic tumor model. NCI-ADR RES cells were implanted i.p. in the SCID mice. Three weeks after of inoculation, mice were treated with either saline, PPT, PTX, PEGylated liposomal doxorubicin (PLD) or Celludo. **A**. Percent survival over time; **B**. Change in body weight over time.

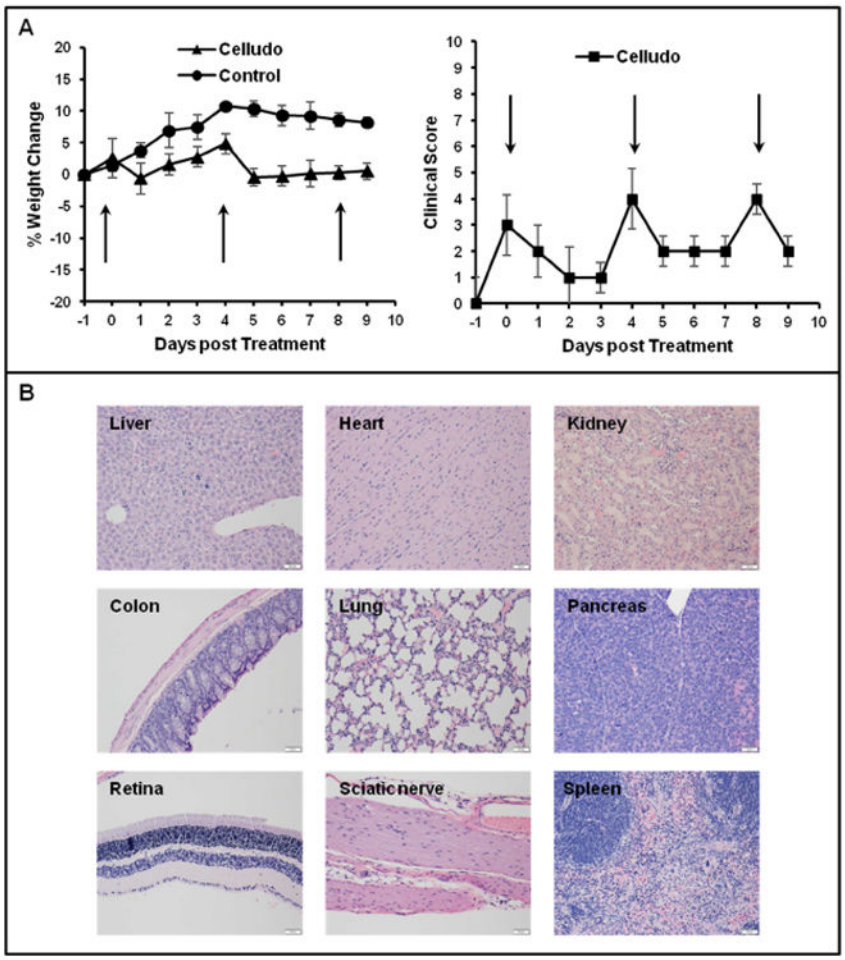

Figure 7.

Clinical observation of mice after treatment with Celludo. **A.** Change in body weight and clinical score upon administration of 3 doses of Celludo (180 mg PPT/kg; day 0, 4 and 8). Results presented as means± SEM, n= 3-4. Mice were clinically scored using an established scoring sheet (supplementary table 1). When the score in a single category reaches 5 or the cumulative score reaches 10 or greater for more than 24 h, the animal would be euthanized. Celludo administrations are indicated with arrows. **B.** Histopathological analysis of different tissues. One day post the final dose, tissues samples were collected, fixed in 10% formalin followed by paraffin embedding, and hematoxylin/eosin staining for histological analysis by a certified animal pathologist.

Table 1

One compartmental pharmacokinetic analysis of free PPT and Celludo in BALB/c mice. *t½:* Half-life. AUC: Area under the curve from 0-240 h. Cl: Clearance. Vd: Volume of distribution. C_0: plasma drug concentration at starting time point. MRT: Mean residence time.

	Celludo	**PPT**
$t_{i/2}$ (h)	11.64	0.66
AUC (μg*h/mL)	45633.70	4.91
CI (mL/h)	0.08	80.94
Vd (mL)	1.33	77.46
C_0 (μg/mL)	2717.00	5.16
MRT(h)	16.80	0.96

Table 2

Biochemical parameters of mice post final injection for control and Celludo treated mice. Results presented as mean± SEM.

Parameters, Units	Hematological parameter following Celludo treatment	
	Control, n=3	Celludo, n=4
WBC, $\times 10^9$ /L	2.4±1.1	1.85±0.5
RBC, $\times 10^{12}$ /L	9±0.3	8.1±0.3
Hemoglobin, g/L	140.7±5.9	122.5±4
Hematocrit, L/L	0.44±0.01	0.38±0.01
MCV, fL	48.3±0.7	46.6±1.2
MCH, pg	15.5±0.2	15.2±0.2
MCHC, g/L	321.3±8.3	329.7±8.4
RDW, %CV	21.6±1.3	20.8±0.6
Platelets, $\times 10^9$ /L	1368.7±203.9	857±134.1
Reticulocyte, %	4.3±0.2	2.9±1.4
Reticulocyte, U L^-	391.7±24.5	177.1±32.2
Neutrophils, %	17±11.5	14.3±9.2
Lymphocytes, %	76.3±14.9	76.8±5.7
Monocytes, %	6.7±4.2	9±3.7

Table 3

Hematological parameters of mice post final injection for control and Celludo treated mice. Results presented as mean± SEM.

Parameters, Units	Biochemical parameter values following injection of various formulations	
	Control, n=3	Celludo, n=4
Glucose, mmol/L	10.1±0.6	11.3±2.3
Urea(BUN), mmol/L	9.8±0.1	8.9±1
Creatinine, umol/L	19.7±7.6	16±4
SDMA, ug/dL	5.7±0.6	7±1.8
Urea(BUN)/Creatinine	138.3±50.5	151.7±56.7
Phosphorus, mmol/L	5.5±2.1	3.5±0.5
Calcium, mmol/L	2.5±0.1	2.6±0.1
Sodium, mmol/L	151	149±0.8
Potassium, mmol/L	8.7±0.5	8.5±0.8
Chloride, mmol/L	110.3±0.6	110±0.8
Bicarbonate, mmol/L	18.6±1.5	16±1.4
Total Protein, g/L	47.7±4.2	51.3±2.6
Albumin, g/L	27.3±1.5	24.8±1.9
Globulin, g/L	20.3±4.5	26.5±2.9
A/G Ratio	1.4±0.4	0.9±0.1
ALT, IU/L	76±72.2	245±232.7
AST, IU/L	80.7±44.5	349.8±255
ALP, IU/L	186.7±9.3	183.3±21.3
T.Bili(Total), umol/L	2.3±0.5	6.1±4.9
CK, IU/L	132.3±69	179.3±135.5